EVIDENCE FOR OLIVINE DEFORMATION IN KIMBERLITES AND OTHER MANTLE-DERIVED MAGMAS DURING CRUSTAL EMPLACEMENT

Version: Revised

Andy Moore[1*], Marina Yudovskaya[2,3], Alexander Proyer[4] Thomas Blenkinsop[5]

[1]Dept. of Geology, Rhodes University, Artillery Road, Grahamstown, South Africa.

[2]Institute of Geology of Ore Deposits, Petrography, Mineralogy and Geochemistry, RAS, 35 Staromonetny, Moscow 119017, Russia

[3]EGRI, University of the Witwatersrand, Private Bag 3, Wits 2050, South Africa

[4]Botswana International University of Science and Technology, Private Bag 16, Palapye, Botswana.

[5]School of Earth and Ocean Sciences, Cardiff University, Cardiff, Wales, U.K. CF10 3XQ

[*]andy.moore.bots@gmail.com (Corresponding author).

Abstract

This paper highlights published and new field and petrographic observations for late-stage (crustal level) deformation associated with the emplacement of kimberlites and other mantle-derived magmas. Thus, radial and tangential joint sets in the competent 183 Ma Karoo basalt wall rocks to the 5 ha. Lemphane kimberlite blow in northern Lesotho have been ascribed to stresses linked to

eruption of the kimberlite magma. Further examples of emplacement-related stresses in kimberlites are brittle fractures and close-spaced parallel shears which disrupt olivine macrocrysts. In each of these examples, there is no evidence of post-kimberlite regional tectonism which might explain these features, indicating that they reflect auto-deformation in the kimberlite during or immediately post-emplacement. On a microscopic scale, these inferred late-stage stresses are reflected by fractures and domains of undulose extinction which traverse core and margins of some euhedral and anhedral olivines in kimberlites and olivine melilitites. Undulose extinction and kink bands have also been documented in olivines in cumulates from layered igneous intrusions. Our observations thus indicate that these deformation features can form at shallow levels (crustal pressures), which is supported by experimental evidence. Undulose extinction and kink bands have previously been presented as conclusive evidence for a mantle provenance of the olivines – i.e. that they are xenocrysts. The observation that these deformation textures can form in both mantle and crustal environments implies that they do not provide reliable constraints on the provenance of the olivines. An understanding of the processes responsible for crustal deformation of kimberlites could potentially refine our understanding of kimberlite emplacement processes.

Introduction

Olivine is always the dominant phase in kimberlites, comprising an average of 50% of the total rock volume (Skinner, 1989). Skinner divided kimberlitic olivines on the basis of size into small, often

euhedral micro-phenocrysts and phenocrysts, <0.5mm in length, and larger (>0.5mm), often anhedral and rounded macrocrysts, often considered to be xenocrysts. Scott-Smith et al (2013) subsequently suggested that the term macrocryst be restricted to olivines > 1.0 mm, but noted that it should be used with a non-genetic connotation. It should be stressed, however, that these sub-divisions are artificial constraints, as kimberlitic olivines typically show a size continuum rather than a bimodal distribution (Moore, 1988; Moss et al., 2010).

There are strongly divergent views on the origin of kimberlitic olivines. Several recent publications have concluded that the cores of all kimberlitic olivines are xenocrysts, derived from disaggregated mantle peridotites, and that only the outer rims crystallized from the host magma (e.g. Kamenetsky et al, 2008; Brett et al., 2009; Arndt et al., 2010; Lim et al., 2018). In contrast, Moore (1988; 2012; 2017) argued that the majority of kimberlitic olivines are cognate phenocrysts. Skinner (1989) took an intermediate view, concluding that the euhedral olivine phenocrysts and microphenocrysts are cognate to the kimberlite, but that the majority of macrocrysts are xenocrysts.

These contrasting interpretations have important implications for the composition and generation of kimberlite magmas. If a majority of olivines are cognate, this would point to a highly Mg-rich primitive kimberlitic liquid, whereas the xenocrystal model implies a carbonatitic, relatively Mg-poor primary magma. It is therefore clearly critical to determine the origin of kimberlite olivines in order

to understand the processes responsible for producing kimberlite magmas.

Various criteria have been proposed to distinguish between a xenocrystal or cognate origin for kimberlitic olivines. Thus, several authors (e.g. Arndt et al., 2010; Bussweiler et al., 2015) note that compositions of the most refractory olivines in kimberlites overlap the range typical of mantle peridotite xenoliths. However, this does not preclude a cognate origin, as the first olivine to crystallize from a magma generated in equilibrium with mantle olivines would be expected to be closely similar in composition to those in the mantle source. Subsequent crystallization would result in decreasing Mg# of the liquidus olivine, but would result in limited initial change in Ni content, as decreasing Mg concentration in the magma would be accompanied by an increase in the Ni partition coefficient (Hart and Davis, 1978; Moore, 2017). The consequence is that olivines produced by fractional crystallization of a magma could, at least in principle, overlap the range of Mg # and Ni concentrations typical of mantle peridotites.

Sharp compositional gradients that are typical of rims of kimberlitic olivines have also been used to argue that the olivine cores are mantle-derived xenocrysts (Bussweiler et al., 2015). However, kimberlites experience complex late-stage P-T-X paths, with rapidly decreasing temperature associated with initiation of fluidization of the magma. Rapidly decreasing temperature would, in turn, result in a sharp increase in K_{Ni} (olivine-liquid) (Matzen et al., 2013), which could account for the steep decrease in Ni which is characteristic of olivine rims (Moore, 2017).

Some (though not all) olivines in mantle peridotites are characterized by internal deformation features, including undulose extinction, kink banding and mosaic recrystallization, which have been ascribed to dynamic stresses in the mantle. Such deformation textures have accordingly been considered to be diagnostic criteria for recognizing mantle-derived olivine xenocrysts (e.g. Skinner, 1989; Scott-Smith et al., 1989; Cordier et al. 2017). Brett et al. (2015) have reported that fractures traversing some olivines terminate at the marginal rind, which they infer to be reflect a late, magmatic overgrowth to a mantle-derived xenocryst.

The purpose of this paper is to highlight published and new field and petrographic observations for late-stage (crustal level) deformation associated with the emplacement of kimberlites. Evidence is presented to demonstrate that olivine deformation textures, which have previously been used to argue for a mantle provenance, can also form in kimberlites and some other mantle-derived magmas in response to stresses associated with emplacement and solidification at crustal depths.

It should be stressed, at the outset, that we are not disputing the existence of olivine xenocrysts in general or a mantle origin for some olivine deformation textures. Rather, if similar textures can

form at shallow (crustal) depths, they do not, on their own, provide reliable evidence for distinguishing whether the olivines have a mantle provenance – i.e. are xenocrysts – or are cognate phenocrysts.

Field evidence for deformation associated with crustal kimberlite emplacement

Previous studies

A study of the Lemphane kimberlite dykes and blows in the northern Lesotho highlands (Kreston, 1973) highlighted exceptionally important, and perhaps overlooked evidence of late-stage (crustal) deformation affecting kimberlite wall rocks. Kreston measured joints in the rigid Karoo basalt wall rocks to the 5.7 ha Lemphane kimberlite blow, and showed that they defined sets that were both tangential (Fig. 1) and radial to the kimberlite margin. The width of the wall rocks affected by these joint sets was not specified, but Kreston observed that they did not persist over any appreciable distance from the Lemphane blow, and were absent in the basalts 25m from the kimberlite contact. As the Karoo basalts of the Lesotho highlands, dated at ~183 Ma. (Marsh et al., 1997), do not show evidence of regional tectonic deformation, Kreston (1973) concluded that the joint sets marginal to the Lemphane blow were linked to stresses that “are obviously caused by the kimberlite”.

Kreston and Dempster (1973) documented a hardebank kimberlite dominated by olivine crystals, with very minor amounts of interstitial serpentine and perovskite, from the Malibamatso dyke swarm (northern Lesotho highlands) (Fig. 2). The kimberlite is traversed by parallel incipient shear zones, and these authors noted that there is a tendency for some of the olivines to show "cleavages" parallel to these lineaments. However, they did not present evidence to show that these partings were crystallographically controlled, and they may be fractures. In view of the absence of evidence for regional deformation post-dating eruption of the Karoo basalt wall rocks, Kreston and Dempster (1973) concluded that both the incipient shears and the cleavages (or fractures) in the olivines developed during the later stages of intrusion of the kimberlite dyke – in other words at crustal levels.

Supporting observations

Figs 3a & 3b illustrate a hand specimen from a kimberlite dyke associated with the Cambrian age (~530 Ma) economic 3 ha Murowa kimberlite pipe, located to the southwest of Masvingo in south-central Zimbabwe (Smith et al., 2004). A majority of olivine macrocrysts in this specimen are characterized by pronounced closely spaced fractures with a sub-parallel alignment, with some showing a second parting set with an oblique orientation.

Micro-faults associated with slickenslides and development of chlorite on the fault plane, were observed in a number of core sections, drilled from surface into the BK16 kimberlite of the Orapa cluster. Fig. 3c illustrates one of these micro-faults. The wall rocks are ~183 Ma Karoo basalts, which do not appear to have been affected by post-eruption deformation.

Fig. 3d illustrates a section of core (hole DTP 12N, 78.3m) from the mid-Cretaceous du Toitspan kimberlite (Kimberley cluster, South Africa), which is traversed by calcite-filled brittle fractures, some of which have disrupted olivine macrocrysts.

Microscopic evidence for late-stage deformation of olivines in kimberlites, olivine melilitites and layered intrusions

Kimberlites

Deformation textures in kimberlitic olivine, when present, are more common in the larger, anhedral

olivines (Skinner, 1989). However, Moore (1988) reported undulose extinction in small euhedral olivines in some kimberlites. This is illustrated by the euhedral olivine from the De Beers kimberlite (Kimberley cluster) in Fig. 4 a & b. The grain exhibits non-uniform extinction domains, some of which extend to the edge of the olivine. Skinner (1989) expressed the view that undulose extinction in euhedral kimberlite olivines is very uncommon, but further in-depth investigation is required to confirm this generalization.

Note that fluid inclusions are present both within the core and margin of the crystal illustrated in Fig. 4a&b, and that fractures traversing the mineral extend to the margins. In Fig. 4c, the core and rim of the largest olivine (top centre) are distinguished by light and dark grey interference colours respectively. Some of the fractures in this olivine also traverse both core and rim. Several of the smaller olivines are also characterized by fractures traversing the whole crystal (e.g. the olivine in the lower right of this image).

The proportions of olivines displaying undulose extinction and other deformation textures seem to vary considerably between kimberlites, but such differences have not been systematically quantified. Thus, Scott-Smith et al (1989) noted that in the Kapamba lamproites (Luangwa Valley, Zambia), undulose extinction was common in both the large anhedral and small euhedral olivines. They observed that this made it difficult to distinguish cognate phenocrysts from exotic xenocrysts.

In contrast, undulose extinction in olivines, including macrocrysts, is absent, subdued or rare in some kimberlites. Examples of kimberlites dominated by relatively undeformed macrocrysts are illustrated by Mitchell (1997) for the Kimberley cluster (Plates 74, 76, 78 & 80); Pipe 200, Lesotho (Plate 84); Vtorogodnitsa, Russia (Plate 86); Lac de Gras, Canada (Plate 90) and Somerset Island, Canada (Plates 94 & 96). However, virtually all of the olivines shown in the flagged images from Mitchell (1997) are characterized by fractures which traverse grain interiors and rims.

Olivine melilitites

Olivine is the dominant phenocryst phase in olivine melilitites from the Namaqualand-Bushmanland area of north-western South Africa. Some crystals are euhedral, with bipyramid terminations and a roughly 2:1 aspect ratio (Fig. 4d). However, many are characterized by re-entrants typical of hopper olivines (Moore and Erlank, 1979), comparable to the magmatic growth forms observed in experimental studies involving a small degree of under-cooling (Donaldson, 1976; Faure et al., 2003)

An example of a “hopper” olivine phenocryst, from the Dikdoorn pipe (Namaqualand) is illustrated in Fig. 4e (PPL) and 4f (XPL).

Figure 5 (data from Moore and Erlank, 1979) illustrates a representative pattern of olivine compositional variation from an olivine melilitite sample from a pipe on the farm Biesiesfontein, in the Namaqualand cluster (Moore & Erlank, 1979). A majority of the olivine cores define a trend of decreasing Mg#, with a relatively small decrease in Ni, and normal outward zonation from the core, except at the very edges, which define a trend of marked reverse zonation. A very subordinate group of olivines with relatively Fe-rich olivine cores are characterized by inverse zonation.

The zonation trend shown by the majority of olivine cores was interpreted by Moore and Erlank (1979) to reflect Raleigh-type crystallization of olivine phenocrysts from the melilitite parental liquid. The reverse zoning defined by the rims was ascribed to late-stage co-precipitation with Fe-oxides, present as intergrowths at the olivine margins. The rare olivines showing inverse zoning are probably related to the Cr-poor megacryst suite (Moore and Costin, 2016).

Layered igneous complexes

Olivines with undulose extinction, kink bands and occasionally granular textures, reflecting recrystallization, have been reported from cumulates from the Lower Zone of the Northern Limb of the Bushveld Igneous Complex (BIC) (Yudovskaya et al, 2013). Examples, taken from this study are

illustrated in Figs. 6g & h. In sample UMT6-1449 (Fig. 6g), the majority of the olivines show undulose extinction. They are characterized by a very restricted compositional range (Mg # 89.85 – 90.02; Ni = 0.147 – 0.152, n = 5; (Yudovskaya et al., 2013). Fig. 6h illustrates kink bands in olivines from a harzburgite cumulate, Zone of the northern limb of the BIC.

Kink-banded olivines have also been described in other crustal complexes such as the Great Dyke (Wilson, 1982), the Poyi ultramafic intrusion (Yao et al., 2017) and Duke Island complex (Li et al., 2012). Yudovskaya et al. (2018) have also reported phlogopite, clinopyroxene, chromite and plagioclase with deformation textures from the northern limb of the BIC.

Discussion

The Lesotho Karoo basalts, dated at ~183 Ma (Marsh et al., 1997), do not show evidence of regional tectonic deformation. Kreston (1973) therefore concluded that the tangential (Fig. 1) and radial joint sets associated with the Lemphane blow are "obviously" caused by emplacement of the kimberlite. The same argument was used by Kreston and Dempster (1973) to conclude that the incipient shears and cleavages (or fractures) in olivines in the Malibamatso dyke must have been developed during the late stages of emplacement of the kimberlite magma – in other words, at crustal levels.

Similar considerations are relevant to account for the close-spaced joint sets traversing the kimberlitic olivines in the Murowa kimberlite dyke, illustrated in Fig. 3 a&b. There is no evidence of regional penetrative deformation of this portion of the Zimbabwe craton subsequent to kimberlite emplacement. It further seems most unlikely that this strong preferred orientation of the olivine joint sets is mantle-derived, as disaggregation of sheared olivines from a mantle xenolith during turbulent transport to the surface would produce a non-systematic orientation pattern. These observations thus provide evidence that development of the close-spaced fracture sets was a response to late-stage stresses within the near solidified kimberlite magma – in other words at crustal levels. Similarly, the absence of post-eruption deformation in the ~183 Ma Karoo basalts forming the wall-rocks to the BK-16 kimberlite in the Orapa cluster (Botswana) indicates that the micro-faults illustrated in Fig. 3c reflect late-stage deformation related to stresses associated with emplacement and cooling of the kimberlite.

The fractures in the Du Toitspan kimberlite , which may disrupt olivine macrocrysts (Fig. 3d), provide evidence for solid state, syn- to post-emplacement deformation of kimberlites, thus precluding their formation as decompression fractures formed within the mantle, such as those reported in some olivines by Brett et al. (2015). The absence of deformation events in the cratonic host country rocks suggests that the latest possible timing of the (auto-)deformation within the kimberlite was

immediately post-emplacement.

Collectively, the field evidence documented show that emplacement of kimberlites is associated with internal stresses that exist over the period of cooling and consolidation of the magma. These stresses must have been of sufficient magnitude to impose the radial and tangential fracture sets on the rigid basalt wall rocks to the Lemphane kimberlite blow, documented by Kreston (1973). Incipient shearing of kimberlites (Fig. 2), development of closely-spaced fracture sets (Fig. 3a&b), minor faults with slickensides (Fig. 3c) and brittle fractures (Fig 3d) are interpreted to reflect a range of responses to internal stresses during and immediately following kimberlite emplacement.

The evidence presented also demonstrates that some kimberlitic olivines experienced fracturing and deformation subsequent to the development of the euhedral crystal margins, and thus during the late stages of kimberlite emplacement (Figs 2 & 3; 4a-c). Thus, undulose extinction and fractures extending from the core to the margin of the euhedral olivine from the de Beers kimberlite (Fig. 4 a&b) point to deformation during the late stages of emplacement and crystallization of the kimberlite magma.

Moore and Erlank (1979) concluded from the study of olivines in the Namaqualand olivine melilitites that the presence of hopper growth forms, indicative of magmatic crystallization, coupled with the

zonation pattern defined by the majority of cores, which is compatible with Raleigh-type crystallization, indicate that the overwhelming majority of olivines in the Namaqualand melilitites have a magmatic origin – i.e. are cognate phenocrysts and not xenocrysts. This interpretation is supported by the absence of olivines with compositions typical of mantle peridotites (Mg # > 89) (Fig. 5). The euhedral olivine from the WAT pipe (Namaqualand Cluster) is characterized by domains of contrasting extinction traversing core and rim of this crystal (Fig. 4d). Similarly, the hopper olivine crystal illustrated in Fig. 4 e & f is characterized by undulose extinction and fractures, both extending from the interior to the margin. The deformation textures illustrated in Figs. 4d-f must therefore reflect post-crystallization deformation at crustal levels.

Collectively, the evidence presented demonstrates that at least some olivines in kimberlites, olivine melilitites and layered complexes have experienced post-crystallization stresses at crustal pressures and temperatures, which have produced strain features similar to those which characterize olivine in some mantle peridotite xenoliths. Thus, we argue that while strain features in olivines, such as undulose extinction, *may* be inherited from a mantle source, they do not provide unambiguous evidence for a mantle provenance. This view is in line with conclusions previously drawn by Yudovskaya et al. (2013) and Yao et al. (2017).

Understanding the detailed origin of the various crustal stress features which we have identified in kimberlites and their wall rocks could potentially provide further insights to the later stages of kimberlite eruption and emplacement. While this is beyond the scope of our primarily descriptive study, we suggest a number of potential processes which should be considered:

A. Kimberlitic wall-rock breccias provide compelling evidence for high energy explosive activity linked to emplacement (Barnett et al., 2011), while Sparks et al. (2006) suggest that kimberlite eruptions may have been Plinian in character. Deformation textures may be linked to stresses transmitted through the magma related to explosive eruption. The radial and concentric structures reported by Kreston may be the result of explosive overpressure and post-explosive underpressure on the pipe walls, as proposed by Nicolaysen and Ferguson (1990). Explosive kimberlite eruption offers a potential explanation for the observation that both small euhedral olivines and large macrocrysts show deformation textures in the Kapamba lamproites (Scott-Smith et al., 1989). However, this may not necessarily always be the case, as olivines with different crystallographic orientations may respond differently to the shock stresses. Also, in individual large macrocrysts, the domains of undulose extinction often have relatively large areas, greater than those of smaller euhedral olivine crystals. This might, in part, account for the rarity of deformation features in smaller olivines.

B. Kreston (1973) suggested that internal kimberlite stresses might be linked to post-explosive torsional forces linked to emplacement of the kimberlite in a plastic or near-solid state.

C. Differential stresses in largely solidified magmas may result from chemical reactions, e.g. a partial serpentinization or carbonation.

D. Stresses may be linked to pressure exerted on solidified kimberlite by the magma from a later pulse of eruption. In general, dynamic conditions in a magmatic plumbing system should result in deformation and brecciation.

Kimberlite deformation linked to one or more of the suggested stresses provides a potential explanation for crustal deformation of olivines. It is noted in this regard that experimental evidence demonstrates that undulose extinction and kink bands can develop in olivines down to very low temperatures (20 – 600 °C), depending on the pressure applied. (Druiventak, et al., 2011). Further, low-Ca olivine tends to be more readily deformed, as high Ca contents in olivine creates the so-called "solute drag" effect, preventing deformations (Yao et al., 2017). The high Ca-contents of kimberlitic micro-phenocryst olivines, and olivine rims would therefore be expected to inhibit plastic deformation.

In addition to the possible mechanisms discussed above, Welsch et al. (2012) have demonstrated that undulose extinction can result directly from crystal growth processes during magmatic crystallization. These authors present evidence that olivine phenocrysts in lava flows associated with the Piton de la Fournaise volcano on Reunion island are composite crystals, formed by parallel dendritic growth with smaller sub-units coalescing to form macrocrysts. However, branch

misorientations and lattice mismatches can sometimes produce sub-grain boundaries, dislocation lamellae and undulose extinction, which they noted have formerly been interpreted in terms of plastic intracrystalline deformation. The undulose extinction in the hopper olivine from the Namaqualand olivine melilitite illustrated in Fig. 3e&f closely matches some of the growth textures documented by Welsch et al. (2012).

Subsolidus deformation in layered igneous complexes may reflect solid state reactions accompanied by increase in volume. This may be linked to exsolution and the formation of sympectites that occur in olivine and pyroxenes. The origin of the exsolutions is controversial (Fleet et al., 1980; Khisina et al., 2013), and their link with deformation is not resolved. Nevertheless, a sub-solidus origin of exsolutions, which are particularly common in grains exhibiting kink bands and undulose extinction, is generally accepted (Yudovskaya et al., 2013, 2018, Yao et al., 2017).

Conclusions

Field and petrographic evidence demonstrate that kimberlites experience a range of stresses during crustal emplacement, extending to early post-solidification of the magma. The processes

responsible for these stresses remain speculative, and an understanding of their origin could potentially refine models for kimberlite emplacement. However, irrespective of their origin, such stresses, possibly coupled with direct crystallization processes, such as those reported by Welsch et al. (2012), provide a potential explanation for late-stage deformation features such as undulose extinction, kink banding and fracturing which we have documented in some olivines.

We stress, once again, that we do not dispute the existence of olivine xenocrysts in general, or a mantle origin for some olivine deformation textures. Nevertheless, our study demonstrates that deformation textures in olivine cannot be used as a reliable indicator of a mantle provenence – i.e. that olivines showing these deformation textures are invariably xenocrysts.

Acknowledgements

Peter Kreston is thanked for permission to publish the images presented in Figs. 1 & 2, and Dr. Frieder Reichardt for providing the Murowa dyke sample illustrated in Fig. 3a&b. The core sample illustrated in Fig. 3d was kindly provided by Petra Diamonds Ltd. Tsodilo Resources (a Canadian-listed diamond exploration company), kindly facilitated a field visit to the company's BK16 kimberlite, located in the mid-Cretaceous (~90 Ma) Orapa pipe cluster in central Botswana. Susan Abraham is thanked for help in producing the diagrams.

References

Arndt NT, Guitreau M, Boullier A-M, Le Roex A. Tomassi A, Cordier P. Sobolev A (2010) Olivine and the origin of kimberlite. J Petrol 51: 573-602

Barnett WP, Kurszlaukis S, Tait M, Dirks P (2011) Kimberlite wall-rock fragmentation processes: Venetia K08 pipe development. Bull Volcanol 73: 941-958

Brett RC, Russell, JK, Andrews GDM, Jones TJ (2015) The ascent of kimberlites: insights from olivine. Earth Planet Sci Let 424: 119-131

Brett RC, Russell JK, Moss S (2009) Origin of olivine in kimberlite: phenocryst or imposter. Lithos 112S: 201-212

Bussweiler Y, Foley SF, Prelević D, Jacob DE (2015) The olivine macrocryst problem: new insights from minor and trace element compositions of olivine from the Lac de Gras kimberlites, Canada. Lithos 220-223: 238-252

Cordier C, Sauzeat , Arndt NT, Boullier A-M, Batanova V, Barou F (2017) Quantitative modelling of the apparent decoupling of Mg# and Ni in kimberlitic olivine margins: a reply to the comment on Cordier *et al.* (2015) by A. Moore. J Petrol 58: 391-393

Donaldson CH (1976) An experimental investigation of olivine morphology. Contrib Mineral Petrol

57: 187-213

Druiventak A, Trepmann CA, Renner J, Hanke K (2011). Low-temperature plasticity of olivine during high stress deformation of peridotite at lithospheric conditions – an experimental study. Earth Planet Sci Lett 311: 199-211.

Faure F, Trolliard G, Nicollet C, Montel J-M (2003) A developmental model of olivine morphology as a function of the cooling rate and the degree of undercooling. Contrib Mineral Petrol 145: 251-263

Fleet ME, Bilcox GA, Barnett R L (1980) Oriented magnetite inclusions in pyroxenes from the Grenville province. Canad Mineral18: 89-99

Hart SR and Davis KE (1978) Nickel partitioning between olivine and silicate melt. Earth Planet Sci Lett 40: 203-219

Kamenetsky VS, Kamenetsky MB, Sobolev AB, Golovin A, Demouchy S, Faure K, Sharygin VV, Kuzmin DV (2008) Olivine in the Udachnaya-east kimberlite (Yakutia, Russia): Types, compositions and origins. J Petrol 49: 823-839

Khisina, NR, Wirth R, Abart R, Rhede D, Heinrich W (2013) Oriented chromite–diopside symplectic inclusions in olivine from lunar regolith delivered by “Luna_24” mission. Geochim. Cosmochim. Acta 104: 84–98.

Kreston P. (1973) The geology of Lemphane pipes and neighbouring intrusions. In: Nixon, PH (ed.). Lesotho Kimberlites, Cape and Transvaal Printers, pp159-167.

Kreston P, Dempster AN (1973) The geology of Pipe 200 and the Malibamatso dyke swarm. In: Nixon, PH (ed.). Lesotho Kimberlites, Cape and Transvaal Printers, pp172-179.

Li C, Thakurta J, Ripley EM (2012) Low-Ca contents and kink-banded textures are not unique to mantle olivine: evidence from the Duke Island complex, Alaska. Mineralogy and Petrology 104:147–153.

Lim E, Giuliani A, Phillips D, and Goemann K (2018) Origin of complex olivine zoning in olivine from diverse, diamondiferous kimberlites and tectonic settings: Ekati (Canada), Alto Paranaiba (Brazil) and Kaalvallei (South Africa). Mineralogy and Petrology S112 suppl. 2: S549 – S554.

Marsh JS, Hooper PR, Rehacek J, Duncan RA Duncan AR (1997) Stratigraphy and age of Karoo basalts of Lesotho and implictions for correlations within the Karoo igneous Province. American Geophysical Union, Monograph 100, Large igneous provinces: continental, oceanic and planetary flood basalts, pp247-272

Matzen AK, Baker BM, Beckett JR, Stolper EM (2013) The temperature and pressure dependence of nickel partitioning between olivine and silicate melt. J Petrol 54: 2521-2545

Mitchell RH (1997) Kimberlites, orangeites lamproites, melilitites and minettes – a petrographic atlas. Almaz Press, Thunder Bay, 243pp.

Moore AE (1988) Olivine: a monitor of magma evolutionary paths in kimberlites and olivine melilitites. Contrib Mineral Petrol 99: 238-248.

Moore AE (2012). The case for a cognate, polybaric origin for kimberlitic olivines. Lithos 128: 1-10.

Moore, AE (2017) Quantitative modelling of the apparent decoupling of Mg# and Ni in kimberlitic olivine margins: Comment on “Cordier et al., Metasomatism of the Lithospheric mantle…” (Journal of Petrology, 56, 1775-1796, 2015). J Petrol 58: 385-390

Moore AE Costin, G (2016) Kimberlitic olivines derived from the Cr-poor and Cr-rich megacryst suites. Lithos 258-259: 215-227

Moore AE, Erlank AJ (1979). Unusual olivine zoning: evidence for complex physico-chemical changes during the evolution of olivine melilitite and kimberlite magmas. Contrib Mineral Petrol 70: 391-405

Moss S, Russell JK, Scott-Smith BH, Brett R (2010) Olivine crystal size distribution in kimberlites. Am Mineral 95: 527-536

Nicolaysen LO, Ferguson J (1990) Cryptoexplosion structures, shock deformation and siderophile concentration related to explosive venting of fluids associated with alkaline ultramavfic magmas. Tectonophysics 171: 303-335

Scott-Smith BH, Skinner, EMW, Loney PE (1989) The Kapamba lamproites of the Luangwa Valley,

eastern Zambia. In: Ross, J. et al. (eds) Proceedings of the 4th International Kimberlite Conference, vol. 1, Geological Society of Australia Special Publication 14: 189-205

Skinner EMW (1989) Contrasting Group I and Group II kimberlite petrology: towards a genetic model for kimberlites. In: Ross, J. et al. (eds) Proceedings of the 4th International Kimberlite Conference, vol. è1, Geological Society of Australia Special Publication 14: 528-544

Smith CB, Sims K, Chimuka L, Duffin A, Beard AD, Townsend R. (2004). Kimberlite metasomatism at Murowa and Sese pipes, Zimbabwe. Lithos 76: 219-232

Sparks RSJ, Baker L, Brown RJ, Field M, Schumacher J, Stripp G, Walters A (2006) J Volcanol Geothermal Res 155: 18-48

Welsch B, Faure F, Famin V, Baronnet A, Bachèlery P (2012) Dendritic crystallization: a single process for all the textures of olivine in basalts. J Petrol 54: 539-574

Wilson, AH, (1982) The geology of the Great Dyke, Zimbabwe: the ultramafic rocks: Journal of Petrology 23: 240–292

Yao Z, Qin K, Xue S (2017) Genetic relationship between deformation and low-Ca content in olivine from magmatic systems: evidence from the Poyi ultramafic intrusion, NW China Mineralogy and Petrology 111: 909–919

Yudovskaya MA, Kinniard JA, Sobolev A., Kuzmin DV, McDonals I, Wilson AH (2013) Petrogenesis of

the Lower Zone, olivine-rich cumulates beneath the Platreef and their correlation with the recognized occurrences in the Bushveld Complex. Economic Geology, 108: 1923-1952.

Yudovskaya M, McCreesh M, Costin G Kinnaird JA (2018) Spinel symplectites and associated reactive textures throughout the Bushveld magmatic section. Abstracts of the 13th International Platinum Symposium, 30 June -7 July 2019, Polokwane, South Africa.

FIGURE CAPTIONS

Fig. 1. Jointing in Karoo basalt parallel to the contact with the Lemphane blow (Northern Lesotho). Arrow marks the actual contact (From Kreston and Dempster, 1973, Plate 44b, and included with permission of Peter Kreston, 2018).

Fig. 2 Incipient shearing in the olivine-rich Rabele Dyke 166, Malibamatso Dyke swarm, northern Lesotho highlands. Note the partings (cleavages or fractures), sub-parallel to the incipient shear zones in some, though not all, of the olivine macrocrysts. (From Kreston and Demster, 1973, Plate 45B, included with permission of the first author.)

Fig 3a. Inferred fractures with a strong preferred orientation in olivines from a dyke in the Murowa kimberlite cluster, central Zimbabwe. Diameter of coin = 25 mm. Sample kindly provided by Dr. Frieder Reichardt.

Fig. 3b. Detail of the sample illustrated in Fig. 3a

Fig. 3c. Slickensides associated with chlorite development on a micro-fault cutting a section of core from the Tsodilo Resources BK16 kimberlite, Orapa Cluster, Central Botswana. Diameter of coin: 18mm.

Fig. 3d Brittle fractures in a core section from the Du Toitspan kimberlite, kindly provided by Petra Diamonds. Note disruption of two olivine macrocrysts by the left-hand vein. The fractures are calcite-filled, except where they disrupt the olivine macrocrysts, and contain serpentine. Diameter of coin: 20mm

Fig. 4a. Equant, euhedral olivine from the de Beers Kimberlite, Kimberley pipe cluster (PPL).

Fig. 4b illustrates the same olivine in XPL. Note the abundance of fluid inclusions in both the interior

509 and margins of the crystal, the fractures, which traverse the olivine interior to margin, and the non-
510 uniform extinction.

511 Fig. 4c. Euhedral olivine phenocryst (upper centre) from the de Beers Kimberlite (Kimberley cluster,
512 South Africa) with the contrasting grey tone interference colours reflecting sharp compositional
513 differences between core and rim (XPL). The shape of the core is slightly rounded, with minor
514 embayments at the bottom. Note the equant shapes of the associated euhedral micro-phenocrysts,
515 and fractures traversing grain interiors and margins of a majority of the olivines.

516 Fig. 4d. Euhedral olivine phenocryst from the WAT olivine melilitite, Namaqualand cluster, South
517 Africa, with domains of contrasting extinction which traverse the core and rim of this crystal (XPL).

518 Fig. 4e. Hopper olivine in the Dikdoring olivine melilitite, Namaqualand, NW South Africa (PPL).

519 Fig. 4f (XPL) illustrates the domains of non-uniform extinction traversing core to rims of this olivine.

520 Fig. 4g . Olivines showing undulose extinction in dunite cumulate (UMT6-1449) from the northern
521 limb of the BIC (from Yudovskaya et al., 2013).

522 Fig. 4h. Kink –banding in olivine from a harzburgite cumulate, northern limb of the BIC (image by M.
523 Yudovskaya).

524

525 Fig. 5 (Data from Moore & Erlank, 1979). Olivines from the olivine melilitite designated BIES, from
526 the farm Biesiesfontein, Namaqualand pipe cluster, north-western South Africa. Circles: olivine
527 cores; squares: olivine rims. Diamond and star reflect a very subordinate population which show

inverse core–to-margin zonation.

Click here to access/download;Figure;Fig. 1-I
jointing.jp

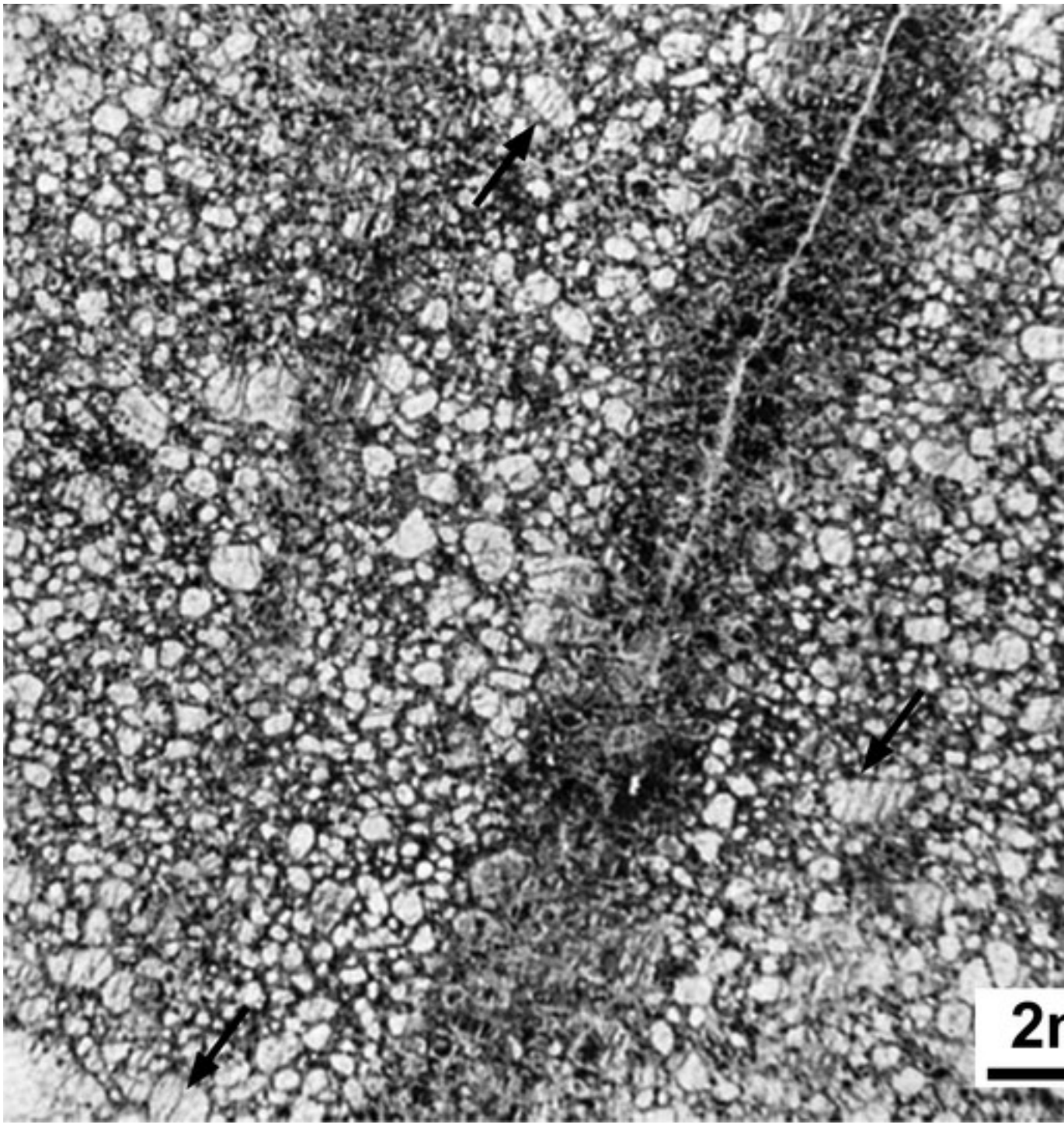
2r


a

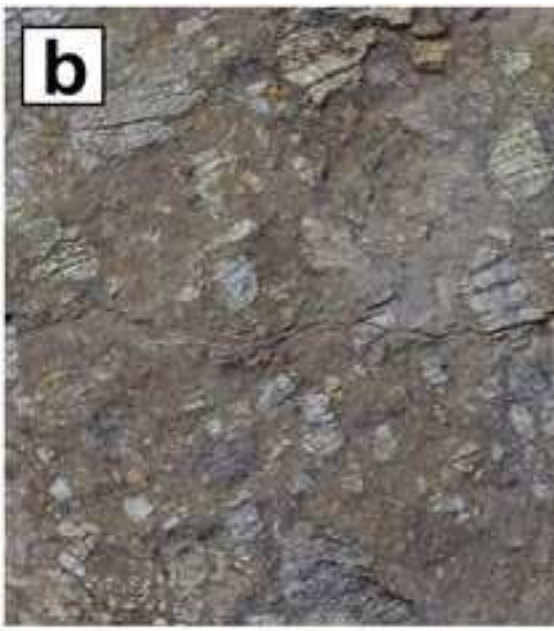
b


c


d

Click here to access/download;Figure;Fig. 4 Olivine paper.jpg

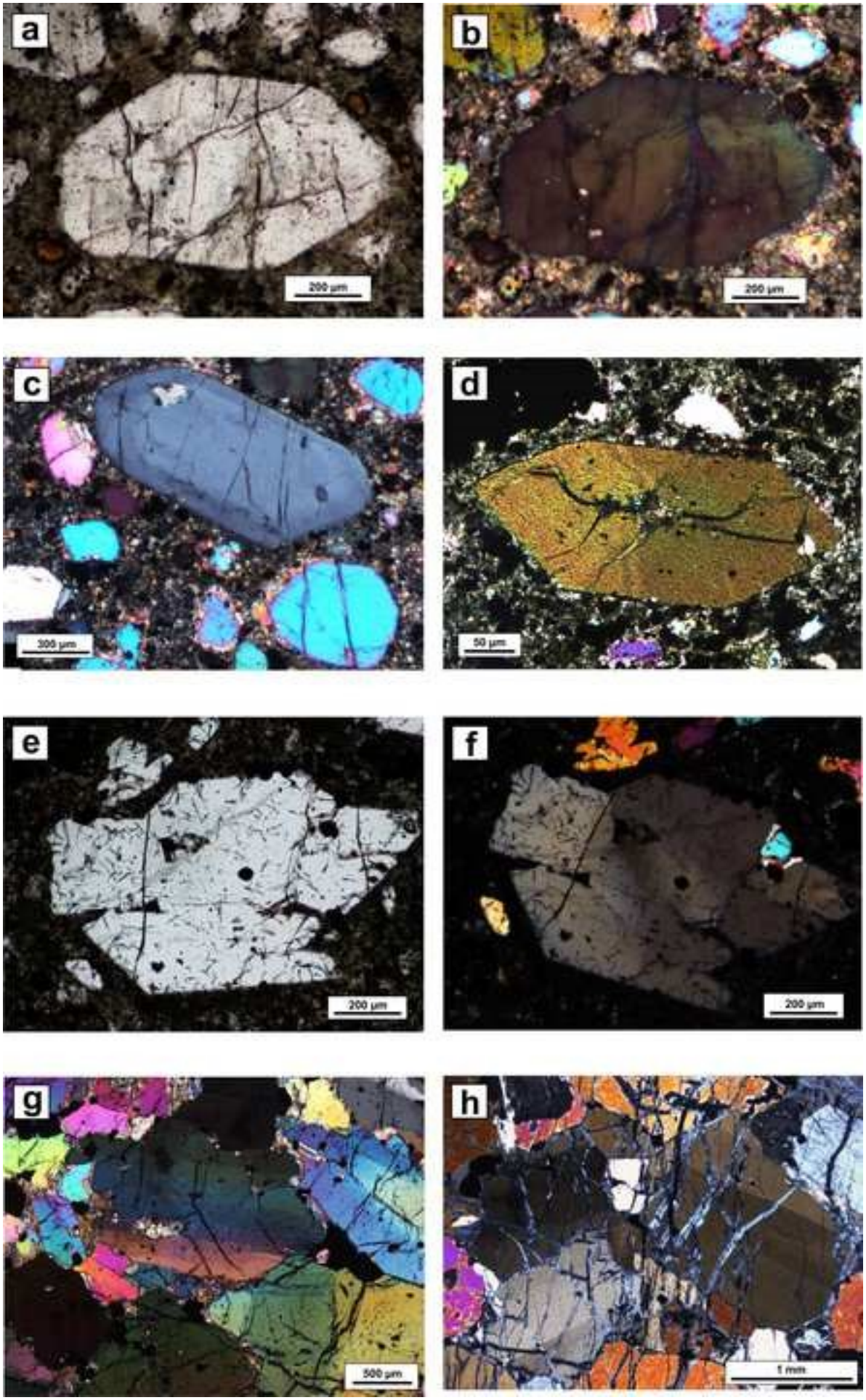
a
200 µm
b
200 µm
c
300 µm
d
50 µm
e
200 µm
f
200 µm
g
500 µm
h
1 mm

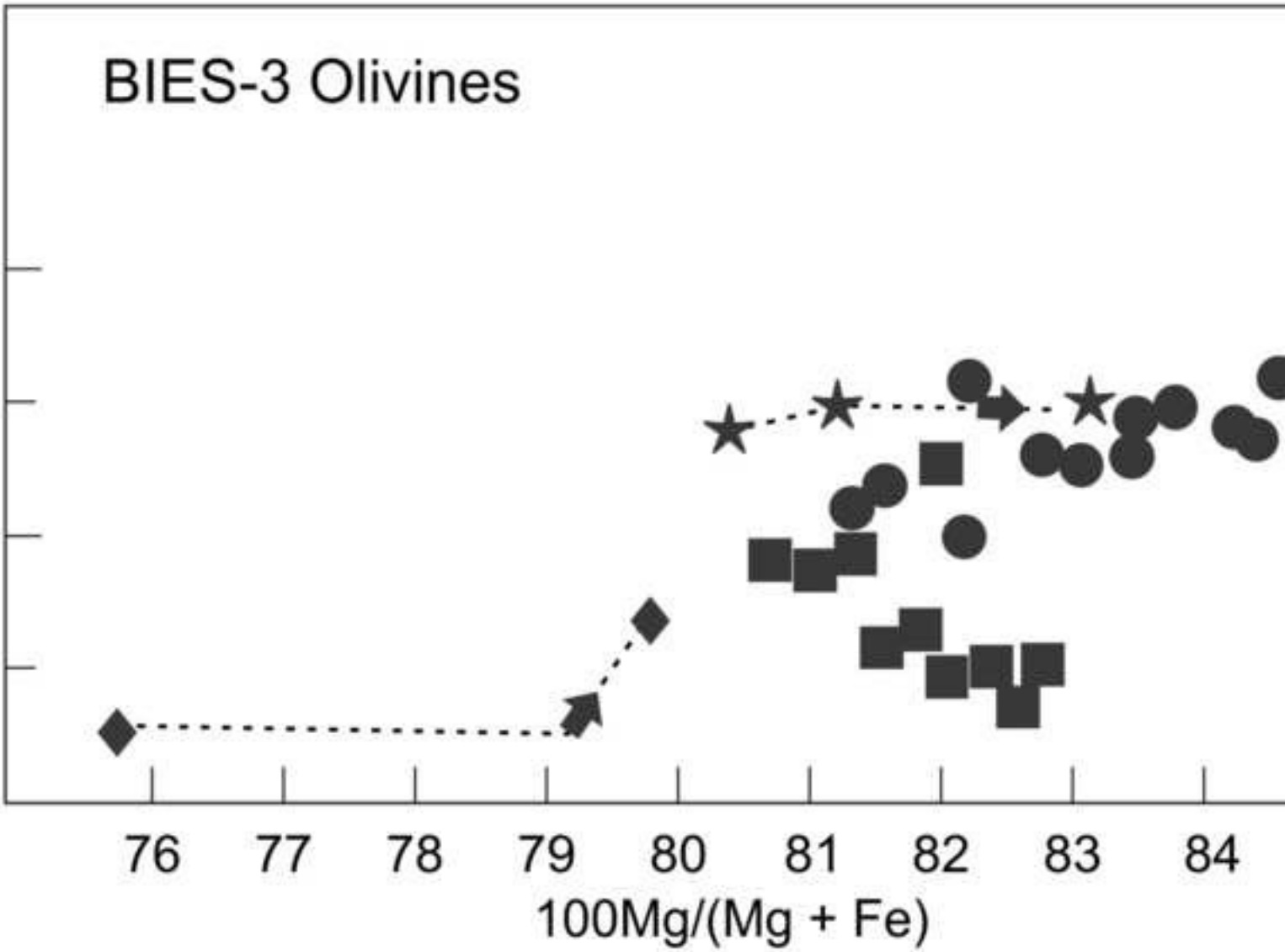
BIES-3 Olivines
76
77
78
79
80
81
82
83
84
100Mg/(Mg + Fe)